

Learning-based model augmentation with LFRs

Jan H. Hoekstra¹, Chris Verhoek¹, Roland Tóth^{1,2}, and Maarten Schoukens¹

¹ Control Systems Group, Eindhoven University of Technology, The Netherlands

² Systems and Control Laboratory, Institute for Computer Science and Control, Budapest, Hungary
j.h.hoekstra@tue.nl, c.verhoek@tue.nl, r.toth@tue.nl, m.schoukens@tue.nl

Abstract—*Artificial neural networks (ANN) have proven to be effective in dealing with the identification nonlinear models for highly complex systems. To still make use of the prior information available from baseline models derived from, e.g., first-principles (FP), methods have been developed that integrate the prior knowledge into the identification algorithm for the ANN in a variety of methods. These methods have shown better estimation speeds and/or accuracy on unseen data. Among these methods are model augmentation structures. A variety of these structures have been considered in literature, there is however no unifying theory to these. In this paper, we propose a flexible linear-fractional-representation (LFR) based model augmentation structure. This model structure is able to represent many common model augmentation structures, thus unifying them under the proposed model structure. Furthermore, we introduce an identification algorithm capable of estimating the proposed model augmentation structure. The performance and generalization capabilities of the identification algorithm and the augmentation structure is demonstrated on a hardening mass-spring-damper simulation example.*

I. INTRODUCTION

With the increasing complexity and performance requirement of systems used in control, the need for accurate nonlinear models of system in practice capturing often complicated behaviors is rapidly growing. Obtaining these models through *first-principles* (FP) based methods is becoming too costly and often infeasible due to the surge of system complexity and difficult to model phenomena for which no reliable FP descriptions exist. Data-driven techniques have appeared to address this modelling challenge in terms of system identification. Especially, recently *artificial neural networks* (ANN) have shown to be able to capture complicated nonlinear dynamic relationships and cope with the high system complexity. For control applications, ANN *state-space* (SS) models [1], [2] are particularly attractive, and with the recent introduction of encoder-based methods such as [3]–[5], estimation of them can be reliably and computationally efficiently accomplished in practice.

To still make use of the prior information available from baseline models derived from, e.g., FP, methods have been developed that integrate the prior knowledge into the identification algorithm for the ANN in a variety of methods [6]. These methods have shown better estimation speeds and/or accuracy on unseen data when a baseline model is used in

the identification procedure. This can be obtained through, e.g., modifying the cost function or model augmentation structures [7]–[9].

In the model augmentation approach, the baseline model is augmented with additional parameterized functions. Unlike other forms of baseline model inclusion methods, this avoids having to relearn the already known relationships that are present in the baseline model. This also means that some dynamics of the identified model will already be known, which could allow for more understandable identified models, in addition to the aforementioned benefits of model augmentation. This method has strong similarities to the grey-box identification method [10] that has been used in system identification with success.

There are a variety of model augmentation structures presented in the literature, such as series [11]–[13], parallel (also known as residual) [12], [13] and mixed [14] augmentation structures. These can be combined with, e.g., cost function modifications [7]. The series and parallel augmentation structures are well established methods, they are however not very flexible in the way augmentation functions can interact with the baseline model, nor do they allow for two way augmentation between the baseline model and the augmentation functions. Mixed model structures do allow for two way interaction between the baseline model and the augmentation functions via the state of the baseline model. These implementations are however often ad hoc. An interesting implementation of the mixed augmentation structure is the *linear-fractional-representation* (LFR) [15], [16]. This model structure has been shown to be useful for robust control [17] and linear parameter varying-control [18], [19].

We propose an LFR-based model augmentation structure that combines a baseline model with augmentation functions in a flexible manner. In the proposed model augmentation structure, an interconnection matrix governs the signals between the baseline model and augmentation functions. By shaping this interconnection matrix, we are able to represent a wide range of model augmentation structures proposed in the literature [7], [11]–[13], [15], [20] resulting in a unifying model structure represented in LFR form. Furthermore, an identification algorithm is developed capable of estimating ANN implementations of the proposed model augmentation structure. Our contributions can be summarized as follows:

- LFR-based model augmentation structure unifying existing model augmentation structures
- System identification algorithm capable of estimating

This work is funded by the European Union (Horizon Europe, ERC, COMPLETE, 101075836). Views and opinions expressed are however those of the author(s) only and do not necessarily reflect those of the European Union or the European Research Council Executive Agency. Neither the European Union nor the granting authority can be held responsible for them.

ing ANN implementations of the proposed LFR-based model augmentation structure.

The remainder of the paper first introduces the system class and baseline model in Section II, followed by the introduction of the LFR-based model augmentation structure in Section III. Next, we show how the proposed model augmentation structure can be used to describe existing augmentation structures in Section IV, followed by an identification algorithm for the proposed augmentation structure in Section V. A hardening *mass-spring-damper* (MSD) simulation example is used to demonstrate the performance of the proposed identification method and compared to a standard ANN-SS method in Section VI. Conclusions are given in Sec VII.

II. SYSTEM CLASS AND BASELINE MODEL

We consider the data generating *discrete-time* (DT) nonlinear system of the form

$$x_{k+1} = f(x_k, u_k), \quad (1a)$$

$$y_k = h(x_k) + e_k, \quad (1b)$$

where $x_k \in \mathbb{R}^{n_x}$ is the state, $u_k \in \mathbb{R}^{n_u}$ is the input, $y_k \in \mathbb{R}^{n_y}$ is the output signal of the system at time moment $k \in \mathbb{Z}$ with e_k an i.i.d., possibly colored, noise process with finite variance representing measurement noise. The state-transition function $f: \mathbb{R}^{n_x} \times \mathbb{R}^{n_u} \rightarrow \mathbb{R}^{n_x}$ and output function $h: \mathbb{R}^{n_x} \rightarrow \mathbb{R}^{n_y}$ are bounded functions. A data sequence generated by (1) is denoted by $\mathcal{D}_N = \{(y_k, u_k)\}_{k=1}^N$.

A baseline model for this DT nonlinear system can for example be obtained by FP methods. The baseline model is assumed to be a fixed model, given as

$$\tilde{x}_{k+1} = f_{\text{base}}(\tilde{x}_k, u_k), \quad (2a)$$

$$\tilde{y}_k = h_{\text{base}}(\tilde{x}_k, u_k), \quad (2b)$$

where $\tilde{x}_k \in \mathbb{R}^{n_{\tilde{x}}}$ is the baseline model state, $\tilde{y}_k \in \mathbb{R}^{n_y}$ the baseline model output, and f_{base} and h_{base} are the baseline model functions for state-transition and output respectively. These are jointly denoted as ϕ_{base} .

III. LFR-BASED AUGMENTATION OF FP MODELS

We augment the baseline model (2) with parameterized augmentation functions, jointly denoted by ϕ_{aug} . The parameters of these functions are given by the parameter vector θ . The proposed LFR-based augmentation structure that combines the ϕ_{base} and ϕ_{aug} is shown in Fig. 1 and can be written as

$$\begin{bmatrix} \hat{x}^+ \\ \hat{y} \\ z_1 \\ z_2 \end{bmatrix} = \underbrace{\begin{bmatrix} S_{xx} & S_{xu} & S_{xw_1} & S_{xw_2} \\ S_{yx} & S_{yu} & S_{yw_1} & S_{yw_2} \\ S_{z_1x} & S_{z_1u} & S_{z_1w_1} & S_{z_1w_2} \\ S_{z_2x} & S_{z_2u} & S_{z_2w_1} & S_{z_2w_2} \end{bmatrix}}_{\mathbf{S}} \begin{bmatrix} \hat{x} \\ u \\ w_1 \\ w_2 \end{bmatrix} \quad (3a)$$

$$w_1 = \phi_{\text{base}}(z_1) = \begin{bmatrix} f_{\text{base}}(z_1) \\ h_{\text{base}}(z_1) \end{bmatrix} \quad (3b)$$

$$w_2 = \phi_{\text{aug}}(z_2), \quad (3c)$$

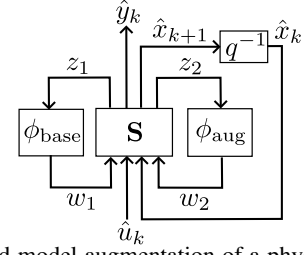


Fig. 1: LFR-based model augmentation of a physical model rewritten as an interconnection structure.

where $\hat{x} \in \mathbb{R}^{n_{\hat{x}}}$ is the model state, $\hat{y} \in \mathbb{R}^{n_y}$ is the model output, $\mathbf{S} \in \mathbb{R}^{n \times m}$ is the interconnection matrix, and S are selection matrices of appropriate size. We use the $+$ symbol to denote time $k+1$ and drop the subscript k for notational convenience.

The model state \hat{x} is given as $\begin{bmatrix} \bar{x}^\top & \bar{x}^\top \end{bmatrix}^\top$, where \bar{x} is the additional state that is added for dynamic augmentation structures. Not all model augmentation structures have such a state \bar{x} . If the model structure does have an augmentation model state, it is considered a dynamic augmentation and otherwise it is a static augmentation.

By choosing different structures for ϕ_{aug} and shaping the selection matrices S , a large variety of augmentation structures can be represented. In Sec. IV we show the procedure to obtain these selection matrices S for a variety of model augmentation structures commonly used in the literature.

A. Conditions on the interconnection matrix

Care needs to be taken with the formulation of the LFR-based model augmentation structure to avoid algebraic loops that lead to well-posedness issues. For a given LFR-based model augmentation structure (3), the presence of algebraic loops can be checked by the lower right submatrix of the interconnection matrix \mathbf{S} consisting of the selection matrices $S_{z_1w_1}$, $S_{z_1w_2}$, $S_{z_2w_1}$ and $S_{z_2w_2}$. Consider this submatrix as an adjacency matrix of a directed graph. If this graph is acyclic then no algebraic loop is present in model augmentation structure. The acyclic property is checked by examining the diagonal elements of the transitive closure of the adjacency matrix. If these elements are zero then the matrix is acyclic.

B. Initialization and normalization

For training of neural networks, normalization of the input and output data to zero mean and to a standard deviation of 1 has shown to improve model estimation [21]. Therefore, the LFR-based model augmentation structure is normalized as in [3], while the augmentation functions are initialized as in [15]. This means that \hat{x} , u , \hat{y} in (3) are normalized. The to-be-augmented baseline model thus needs to have normalized input, state and output as well. This is accomplished by the following transformation

$$\tilde{f}_{\text{base}} = T_x f_{\text{base}}(T_x^{-1} \tilde{x}, T_u^{-1} u) \quad (4a)$$

$$\tilde{h}_{\text{base}} = T_y h_{\text{base}}(T_x^{-1} \tilde{x}, T_u^{-1} u), \quad (4b)$$

where $T_u \in \mathbb{R}^{n_u}$ is a diagonal matrix with the inverse of the standard deviation (taken over the samples) of denormalized input u on its diagonal. T_y is similarly defined with measurements of output y . For T_x , the standard deviation is determined over the baseline model states \tilde{x} . These states can be obtained by, e.g., simulation of the baseline model with nominal input and initial conditions.

IV. AUGMENTATION STRUCTURES

To demonstrate the flexibility of the proposed LFR-based model augmentation structure (3), we show how it can be used to represent six common model augmentation structures found in the literature [6], [7], [11]–[13], [15], [16], [20]. These are the parallel, series and mixed augmentation structures in both the static and dynamic case. The dynamic cases are shown in Fig. 2. The static cases can be retrieved from the dynamic cases by removing the augmentation state \tilde{x} . We proceed by rewriting both the static and dynamic cases to an equation form for the progressed baseline state \tilde{x} , progressed augmentation state \tilde{x}^+ and model output \hat{y} . The resulting equations are shown in Table I. In this table, f_0 and h_0 are used instead of f_{base} and h_{base} , and the remaining functions are part of the parameterized augmentation functions ϕ_{aug} . We proceed by showing how for the dynamic cases in Table I the selection matrices S in (3) can be obtained.

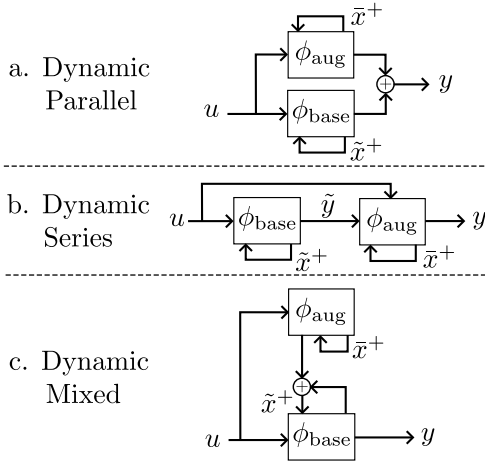


Fig. 2: Model structures of parallel, series and state augmentation.

A. Dynamic parallel augmentation

The first model augmentation structure we consider is the parallel output model structure shown in Fig. 2.a. The dynamic parallel model augmentation structure can be formulated into the signals in (3) as

$$\begin{aligned} z_1 &= \text{col} \begin{bmatrix} \tilde{x} & u \end{bmatrix}, & w_1 &= \text{col} \begin{bmatrix} \tilde{x}^+ & \tilde{y} \end{bmatrix} = \phi_{\text{base}}(z_1), \\ z_2 &= \text{col} \begin{bmatrix} \tilde{x} & u \end{bmatrix}, & w_2 &= \text{col} \begin{bmatrix} \tilde{x}^+ & \tilde{y} \end{bmatrix} = \phi_{\text{aug}}(z_2), \\ \tilde{x}^+ &= \begin{bmatrix} I_{n_{\tilde{x}}} & 0^{n_{\tilde{x}} \times n_y} \end{bmatrix} w_1, \\ \tilde{x}^+ &= \begin{bmatrix} I_{n_{\tilde{x}}} & 0^{n_{\tilde{x}} \times n_y} \end{bmatrix} w_2, \\ y &= \begin{bmatrix} 0^{n_y \times n_{\tilde{x}}} & I_{n_y} \end{bmatrix} w_1 + \begin{bmatrix} 0^{n_y \times n_{\tilde{x}}} & I_{n_y} \end{bmatrix} w_2, \end{aligned}$$

where \tilde{y} is the augmentation model output, col is the column vector of the concatenated values, I_n is the identity matrix of

size n , and $0^{m \times n}$ is the zero matrix of size m by n . With these signals, the interconnect matrix in (3) can then be formulated with following matrices

$$\begin{aligned} S_{z_1 x} &= \begin{bmatrix} I_{n_{\tilde{x}}} & 0^{n_{\tilde{x}} \times n_{\tilde{x}}} \\ 0^{n_u \times n_{\tilde{x}}} & 0^{n_u \times n_{\tilde{x}}} \end{bmatrix}, & S_{z_1 u} &= \begin{bmatrix} 0^{n_{\tilde{x}} \times n_u} \\ I_{n_u} \end{bmatrix}, \\ S_{z_2 x} &= \begin{bmatrix} 0^{n_{\tilde{x}} \times n_{\tilde{x}}} & I_{n_{\tilde{x}}} \\ 0^{n_u \times n_{\tilde{x}}} & 0^{n_u \times n_{\tilde{x}}} \end{bmatrix}, & S_{z_2 u} &= \begin{bmatrix} 0^{n_{\tilde{x}} \times n_u} \\ I_{n_u} \end{bmatrix}, \\ S_{xw_1} &= \begin{bmatrix} I_{n_{\tilde{x}}} & 0^{n_{\tilde{x}} \times n_y} \\ 0^{n_{\tilde{x}} \times n_{\tilde{x}}} & 0^{n_{\tilde{x}} \times n_y} \end{bmatrix}, & S_{xw_2} &= \begin{bmatrix} 0^{n_{\tilde{x}} \times n_{\tilde{x}}} & 0^{n_{\tilde{x}} \times n_y} \\ I_{n_{\tilde{x}}} & 0^{n_{\tilde{x}} \times n_y} \end{bmatrix}, \\ S_{yw_1} &= \begin{bmatrix} 0^{n_y \times n_{\tilde{x}}} & I_{n_y} \end{bmatrix}, & S_{yw_2} &= \begin{bmatrix} 0^{n_y \times n_{\tilde{x}}} & I_{n_y} \end{bmatrix}, \end{aligned}$$

with all other matrices in (3) set to zero matrices of appropriate sizes. With these selection matrices S , the interconnection matrix \mathbf{S} can now be constructed. This, in combination with the baseline model ϕ_{base} and the augmentation functions ϕ_{aug} , gives the LFR-based augmentation structure.

B. Dynamic series augmentation

The second model augmentation structure we consider is the dynamic series model structure shown in Fig. 2.b. This model structure can be formulated into the signals in (3) as

$$\begin{aligned} z_1 &= \text{col} \begin{bmatrix} \tilde{x} & u \end{bmatrix}, & w_1 &= \text{col} \begin{bmatrix} \tilde{x}^+ & \tilde{y} \end{bmatrix} = \phi_{\text{base}}(z_1), \\ z_2 &= \text{col} \begin{bmatrix} \tilde{x} & u & \tilde{y} \end{bmatrix}, & w_2 &= \text{col} \begin{bmatrix} \tilde{x}^+ & \tilde{y} \end{bmatrix} = \phi_{\text{aug}}(z_2), \\ \tilde{x}^+ &= \begin{bmatrix} I_{n_{\tilde{x}}} & 0^{n_{\tilde{x}} \times n_y} \end{bmatrix} w_1, \\ \tilde{x}^+ &= \begin{bmatrix} I_{n_{\tilde{x}}} & 0^{n_{\tilde{x}} \times n_y} \end{bmatrix} w_2, \\ y &= \begin{bmatrix} 0^{n_y \times n_{\tilde{x}}} & I_{n_y} \end{bmatrix} w_2. \end{aligned}$$

The interconnect matrix can then be formulated with following matrices

$$\begin{aligned} S_{z_1 x} &= \begin{bmatrix} I_{n_{\tilde{x}}} & 0^{n_{\tilde{x}} \times n_{\tilde{x}}} \\ 0^{n_u \times n_{\tilde{x}}} & 0^{n_u \times n_{\tilde{x}}} \end{bmatrix}, & S_{z_1 u} &= \begin{bmatrix} 0^{n_{\tilde{x}} \times n_u} \\ I_{n_u} \end{bmatrix}, \\ S_{z_2 x} &= \begin{bmatrix} 0^{n_{\tilde{x}} \times n_{\tilde{x}}} & I_{n_{\tilde{x}}} \\ 0^{n_u \times n_{\tilde{x}}} & 0^{n_u \times n_{\tilde{x}}} \\ 0^{n_y \times n_{\tilde{x}}} & 0^{n_y \times n_{\tilde{x}}} \end{bmatrix}, & S_{z_2 u} &= \begin{bmatrix} 0^{n_{\tilde{x}} \times n_u} \\ I_{n_u} \\ 0^{n_y \times n_u} \end{bmatrix}, \\ S_{z_2 w_1} &= \begin{bmatrix} 0^{n_{\tilde{x}} \times n_{\tilde{x}}} & 0^{n_{\tilde{x}} \times n_y} \\ 0^{n_u \times n_{\tilde{x}}} & 0^{n_u \times n_y} \\ 0^{n_y \times n_{\tilde{x}}} & I_{n_y} \end{bmatrix}, \\ S_{xw_1} &= \begin{bmatrix} I_{n_{\tilde{x}}} & 0^{n_{\tilde{x}} \times n_y} \\ 0^{n_{\tilde{x}} \times n_{\tilde{x}}} & 0^{n_{\tilde{x}} \times n_y} \end{bmatrix}, & S_{xw_2} &= \begin{bmatrix} 0^{n_{\tilde{x}} \times n_{\tilde{x}}} & 0^{n_{\tilde{x}} \times n_y} \\ I_{n_{\tilde{x}}} & 0^{n_{\tilde{x}} \times n_y} \end{bmatrix}, \\ S_{yw_2} &= \begin{bmatrix} 0^{n_y \times n_{\tilde{x}}} & I_{n_y} \end{bmatrix}. \end{aligned}$$

This allows for construction of (3).

C. Dynamic mixed augmentation

The third model augmentation structure we consider is the dynamic mixed model structure shown in Fig. 2.c. Compared to the series and parallel augmentations, this state augmentation allows for a 2-way dependency between the baseline model and the augmentation model. The dynamic mixed model structure can be formulated into the signals of in (3) as

TABLE I: Classes of model augmentation structures where f_{base} and h_{base} are denoted as f_0 and h_0

	static parallel	dynamic parallel	static series	dynamic series	static mixed	dynamic mixed
\tilde{x}^+	$f_0(\tilde{x}, u)$	$f_0(\tilde{x}, u)$	$f_0(\tilde{x}, u)$	$f_0(\tilde{x}, u)$	$f_0(\tilde{x}, u) + g_\theta(\tilde{x}, u)$	$f_0(\tilde{x}, u) + g_\theta(\tilde{x}, \tilde{x}, u)$
\tilde{x}^+	-	$f_\theta(\tilde{x}, u)$	-	$f_\theta(h_0(\tilde{x}, u), \tilde{x}, u)$	-	$f_\theta(\tilde{x}, \tilde{x}, u)$
\hat{y}	$h_0(\tilde{x}, u) + h_\theta(\tilde{x}, u)$	$h_0(\tilde{x}, u) + h_\theta(\tilde{x}, u)$	$h_\theta(h_0(\tilde{x}, u), u)$	$h_\theta(\tilde{x}, u)$	$h_0(\tilde{x}, u)$	$h_0(\tilde{x}, u)$

$$\begin{aligned}
 z_1 &= \text{col} \begin{bmatrix} \tilde{x} & u \end{bmatrix}, & w_1 &= \text{col} \begin{bmatrix} \tilde{x}^+ & \tilde{y} \end{bmatrix} = \phi_{\text{base}}(z_1), \\
 z_2 &= \text{col} \begin{bmatrix} \tilde{x} & \tilde{x} & u \end{bmatrix}, & w_2 &= \text{col} \begin{bmatrix} \tilde{x}_g^+ & \tilde{x}^+ \end{bmatrix} = \phi_{\text{aug}}(z_2), \\
 \tilde{x}^+ &= \begin{bmatrix} \mathbf{I}_{n_{\tilde{x}}} & \mathbf{0}^{n_{\tilde{x}} \times n_y} \end{bmatrix} w_1 + \begin{bmatrix} \mathbf{0}^{n_{\tilde{x}} \times n_{\tilde{x}}} & \mathbf{I}_{n_{\tilde{x}}_g} \end{bmatrix} w_2, \\
 \tilde{x}^+ &= \begin{bmatrix} \mathbf{I}_{n_{\tilde{x}}} & \mathbf{0}^{n_{\tilde{x}} \times n_{\tilde{x}}_g} \end{bmatrix} w_2, \\
 y &= \begin{bmatrix} \mathbf{0}^{n_y \times n_{\tilde{x}}} & \mathbf{I}_{n_y} \end{bmatrix} w_1,
 \end{aligned}$$

where \tilde{x}_g^+ is the part of the augmentation model that works on the progressed baseline state \tilde{x}^+ . The interconnect matrix can then be formulated with following matrices

$$\begin{aligned}
 S_{z_1 x} &= \begin{bmatrix} \mathbf{I}_{n_{\tilde{x}}} & \mathbf{0}^{n_{\tilde{x}} \times n_{\tilde{x}}} \\ \mathbf{0}^{n_u \times n_{\tilde{x}}} & \mathbf{0}^{n_u \times n_{\tilde{x}}} \end{bmatrix}, & S_{z_1 u} &= \begin{bmatrix} \mathbf{0}^{n_{\tilde{x}} \times n_u} \\ \mathbf{I}_{n_u} \end{bmatrix}, \\
 S_{z_2 x} &= \begin{bmatrix} \mathbf{I}_{n_{\tilde{x}}} \\ \mathbf{0}^{n_u \times n_{\tilde{x}}} \end{bmatrix}, & S_{z_2 u} &= \begin{bmatrix} \mathbf{0}^{n_{\tilde{x}} \times n_u} \\ \mathbf{I}_{n_u} \end{bmatrix}, \\
 S_{xw_1} &= \begin{bmatrix} \mathbf{I}_{n_{\tilde{x}}} & \mathbf{0}^{n_{\tilde{x}} \times n_y} \\ \mathbf{0}^{n_{\tilde{x}} \times n_{\tilde{x}}} & \mathbf{0}^{n_{\tilde{x}} \times n_y} \end{bmatrix}, & S_{xw_2} &= \mathbf{I}_{n_{\tilde{x}}}, \\
 S_{yw_1} &= \begin{bmatrix} \mathbf{0}^{n_y \times n_{\tilde{x}}} & \mathbf{I}_{n_y} \end{bmatrix}.
 \end{aligned}$$

This allows for construction of (3).

V. ENCODER-BASED ESTIMATION ALGORITHM

Consider again the DT nonlinear system (1). Using a data sequence \mathcal{D}_N generated by (1), we aim to identify the augmented model (3), denoted by ϕ_θ , in the form

$$\begin{bmatrix} \hat{x}_{k+1} \\ \hat{y}_k \end{bmatrix} = \phi_\theta(\hat{x}_k, u_k), \quad (5)$$

where the functions in ϕ_{aug} are feedforward multi-layer artificial neural networks¹ with $\theta \in \mathbb{R}^{n_\theta}$ collecting the activation weights as model parameters. Under these considerations, the model structure (5) represents a recurrent neural network, also called an ANN-SS model [1].

The literature on identifying ANN-SS models is rapidly developing. There are many approaches to identify such models, e.g., [4], [22]. A recent approach that estimates (5) under statistical consistency guarantees is the SUBNET approach [3]. This method has shown state-of-the-art results on multiple identification benchmarks and can be used to estimate models with high-dimensional inputs and outputs [23]. To computationally efficient achieve this estimation, SUBNET uses a truncated simulation error objective function as shown in Fig. 3, which combines multiple subsections of

¹Consider that each hidden layer is composed of m activation functions $\rho: \mathbb{R} \rightarrow \mathbb{R}$ in the form of $z_{i,j} = \rho(\sum_{l=1}^{m_{l-1}} \theta_{w,i,j,l} z_{i-1,l} + \theta_{b,i,j})$ where $z_i = \text{col}(z_{i,1}, \dots, z_{i,m_i})$ is the latent variable representing the output of layer $1 \leq i \leq q$. Here, $\text{col}(\cdot)$ denotes the composition of a column vector. For a f_θ with q hidden-layers and linear input and output layers, this means $f_\theta(\hat{x}_k, u_k) = \theta_{w,q+1} z_q(k) + \theta_{b,q+1}$ and $z_0(k) = \text{col}(\hat{x}_k, u_k)$.

TABLE II: Physical parameters 3 DOF hardening mass-spring-damper system

	Mass m_i	Spring k_i	Damper c_i	Hardening a_i
1	0.5 kg	100 $\frac{\text{N}}{\text{m}}$	0.5 $\frac{\text{Ns}}{\text{m}}$	100 $\frac{\text{N}}{\text{m}^3}$
2	0.4 kg	100 $\frac{\text{N}}{\text{m}}$	0.5 $\frac{\text{Ns}}{\text{m}}$	-
3	0.1 kg	100 $\frac{\text{N}}{\text{m}}$	0.5 $\frac{\text{Ns}}{\text{m}}$	-

length T of the available data \mathcal{D}_N . This objective function is given as

$$V(\theta) = \frac{1}{2N(T+1)} \sum_{i=1}^N \sum_{\ell=0}^{T-1} \|\hat{y}_{k_i|k_i+\ell} - y_{k_i+\ell}\|_2^2 \quad (6a)$$

$$\begin{bmatrix} \hat{x}_{k_i|k_i+\ell+1} \\ \hat{y}_{k_i|k_i+\ell} \end{bmatrix} := \phi_\theta(\hat{x}_{k_i|k_i+\ell}, u_{k_i+\ell}) \quad (6b)$$

$$\hat{x}_{k_i|k_i} := \psi_\theta(u_{k-n_b}^{k-1}, y_{k-n_a}^k), \quad (6c)$$

where $k_i|k_i+\ell$ indicates the state \hat{x}_k or output \hat{y} at time $k_i+\ell$ simulated from the initial state $\hat{x}_{k_i|k_i}$ at time k_i . The subsections start from a randomly selected time $k \in \{n+1, \dots, N-T\}$. The initial state of these subsections is estimated by an encoder function ψ_θ based on past input and output data, i.e., $\hat{x}_{0|k} = \psi_\theta(u_{k-n_b}^{k-1}, y_{k-n_a}^k)$ where $u_k^{k+\tau} = [u_k^\top \dots u_{k+\tau}^\top]^\top$ for $\tau \geq 0$ and $y_k^{k+\tau}$ is defined similarly. This encoder is co-estimated with ϕ_θ .

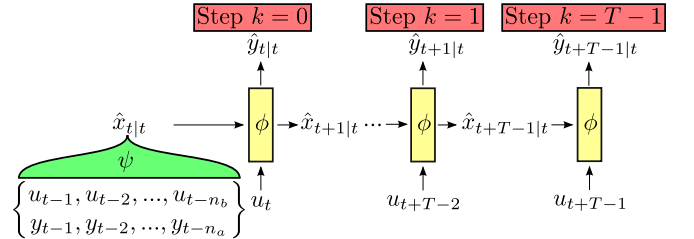


Fig. 3: SUBNET structure: the subspace encoder ψ_θ estimates the initial state at time index k based on past inputs and outputs, then the state is propagated through ϕ_θ multiple times until a simulation length T .

VI. SIMULATION EXAMPLE

For simulation², a 3 degrees-of-freedom (DOF) hardening MSD is considered as shown in Fig. 4 with the physical parameters as given in Table II. The states of the system representation are the positions p_i and accelerations \ddot{p}_i of the masses m_1, m_2, m_3 . The hardening spring with parameter a_1 is connected to mass m_1 . This is a nonlinear cubic spring and thus the system is nonlinear.

We obtain the data for model estimation by applying RK4-based numerical integration on the 3 DOF MSD system

²<https://github.com/Mixxxxx358/Model-Augmentation-Public>

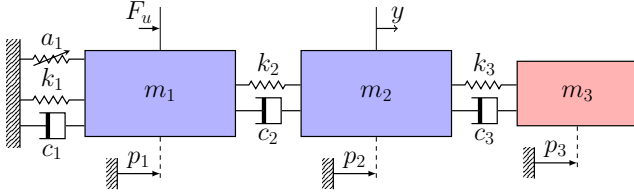


Fig. 4: 3 DOF hardening mass-spring-damper system. The linear dynamics of the m_1 and m_2 are assumed known while the dynamics of m_3 and the contribution of a_1 are unknown.

TABLE III: Normalized root mean square error evaluation of models

Model	NRMS
baseline	35.02%
dynamic series	8.47%
dynamic parallel	17.63%
linear dynamic mixed	5.39%
nonlinear static mixed	0.38%
nonlinear dynamic mixed	0.15%
ANN-SS	1.26%

with $T_s = 0.02s$. The system is simulated for a *zero-order hold* (ZOH) input signal F_u generated by a DT multisine u_k with frequency 1666 components in the range $[0, 25]$ Hz with a uniformly distributed phase in $[0, 2\pi)$. The sampled output measurements y_k are perturbed by additive noise e_k described by a discrete-time white noise process with $e_k \sim \mathcal{N}(0, \sigma_e^2)$. Here σ_e is chosen such that the *signal-to-noise ratio* (SNR) equals 60 dB. After removing the transient due to initial conditions, the sampled generated output y_k for the input u_k is collected in the data sequence \mathcal{D}_N . A separate data sequence is generated for estimation, validation, and testing with size $N_{\text{est}} = 2 \cdot 10^4$, $N_{\text{val}} = 10^4$, $N_{\text{test}} = 10^4$, respectively.

The baseline model is taken as the discretization of the system with $a_1 = 0$ and with $k_3 = 0$, $c_3 = 0$, $m_3 = 0$. Thus the baseline model is linear with 2 DOF. The simulation error of the baseline model on the test data is shown in orange in Fig. 5. As performance measurement of our models we use the *normalized root mean square error* (NRMS) given as

$$\text{NRMS} = \frac{\sqrt{1/N \sum_{k=1}^N \|y_k - \hat{y}_k\|_2^2}}{\sigma_y} \times 100,$$

where σ_y is the standard deviation of the output measurements y . The NRMS of the baseline model is shown in Table III.

Next, we estimate the model augmentation structures shown in Fig. 2, where the augmentation functions are chosen as feedforward neural networks with tanh activation functions. The number of hidden layers and neurons are as in Table IV. For the dynamic series and parallel case we used separate baseline model and augmentation model states, with 6 states for the augmentation model. For the mixed augmentation structure, we consider three different implementations. First, a dynamic mixed augmentation with 2 additional states and linear activation functions. With this augmented model, we expect to be able to capture the dynamics of the third mass missing from the baseline

TABLE IV: Hyperparameters for identifying the augmented model and ANN-SS model.

hidden layers	nodes	n_u n_y	n_a n_b	T	epochs	batch size
2	64	1	7	200	5000	2000

model. Second, a static mixed augmentation with nonlinear activation functions. With this augmented model, we expect to be able to capture the dynamics of the nonlinear spring missing from the baseline model. Third, a dynamic mixed augmentation with 2 additional states and nonlinear activation functions. With this augmented model, we expect to be able to capture all dynamics missing from the baseline model.

The augmented models are estimated as described in Section V with the aforementioned estimation data. The hyperparameters for these estimations are shown in Table IV. As a black-box comparison to the augmented models, an ANN-SS model [3] is estimated with the same estimation procedure and hyperparameters. The NRMS for simulation of the test data using these estimated models are shown in Table III. The nonlinear dynamic mixed augmentation results in the lowest NRMS. The nonlinear static mixed augmentation also results in a low NRMS score, but slightly higher than the nonlinear dynamic mixed augmentation. This is expected for augmentation of a system with missing dynamics that can be represented with additional states. The ANN-SS model results in a higher NRMS than the nonlinear mixed augmentations. We expect, however, that the estimation of the ANN-SS model with a large number of epochs, barring local minima in the estimation process, will result in a model as accurate as the nonlinear dynamic mixed augmentation. This due to the fact that the ANN-SS is a general function approximator. It is however also desirable that the model estimation results in a good estimate in a small number of epochs, since it is not always feasible to train for a large number of epochs, due to, e.g., time or computational limitations.

Next, Fig. 5 shows the simulation error on test data in blue of the nonlinear dynamic mixed augmented model in green and the baseline model in orange. This figure shows that the augmented model is able to perform consistently well across the entire test data.

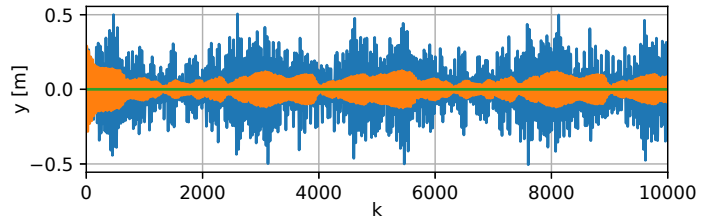


Fig. 5: Simulation error of the baseline model (orange) and nonlinear state augmented model (green) compared to the measured test data (blue).

Finally, Fig. 6 shows the comparison between the states \hat{x} of the nonlinear dynamic mixed model in blue and the part of that state that is contributed by the augmentation

functions in orange. The figure shows that the contribution to the state by the augmentation functions is relatively small for the first four states comprising the baseline model states \bar{x} . The last two states are the additional states \bar{x} added by the augmentation functions and are thus equal to the corresponding model states. From this, we can conclude that the baseline model is in terms of magnitude the dominant factor in the states that are used for the baseline model. The baseline model states are also the states used for the output function, and thus the baseline model states are dominant in the output function. Therefore, we can conclude that the augmentation functions are augmenting the baseline model resulting in an accurate model, and not replacing the baseline model with its own dynamics.

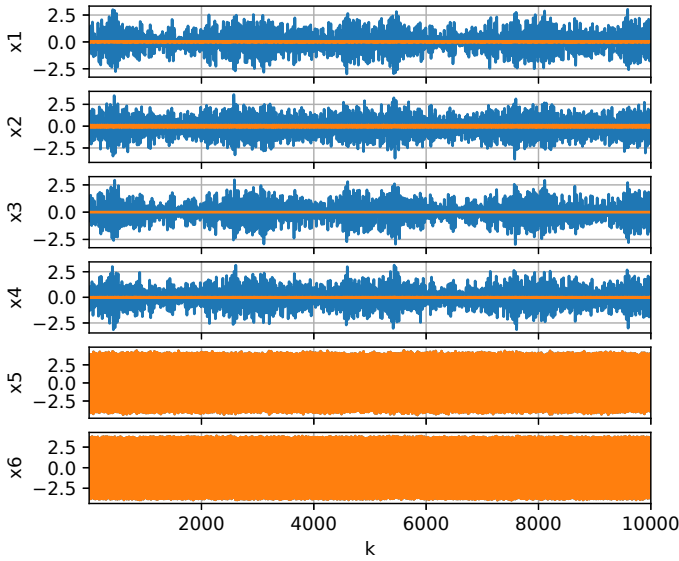


Fig. 6: Comparison between augmented model states (blue) and the contribution to those states by the augmentation model (orange) for a simulation of the augmented model.

VII. CONCLUSION

We have proposed an LFR-based model augmentation structure that flexibly augments baseline models with parameterized augmentation functions. This model augmentation structure unifies a wide range of existing model augmentation structures present in literature. Furthermore, an identification algorithm has been implemented capable of estimating ANN implementations of the proposed model augmentation structure. This identification algorithm has shown to be able to estimate the representations of the many common model augmentation structure present in literature. For the nonlinear mixed dynamic model structure the convergence to an accurate estimated model is faster than the ANN-SS estimation method, without replacing the dynamics of the baseline model.

REFERENCES

[1] J. A. Suykens, B. L. De Moor, and J. Vandewalle, "Nonlinear system identification using neural state space models, applicable to robust control design," *International Journal of Control*, vol. 62, no. 1, pp. 129–152, 1995.

[2] M. Schoukens, "Improved initialization of state-space artificial neural networks," in *Proc. of the 2021 European Control Conference*, 2021, pp. 1913–1918.

[3] G. I. Beintema, M. Schoukens, and R. Tóth, "Deep subspace encoders for nonlinear system identification," *Automatica*, vol. 156, p. 111210, 2023.

[4] M. Forgone and D. Piga, "Continuous-time system identification with neural networks: Model structures and fitting criteria," *European Journal of Control*, vol. 59, pp. 69–81, 2021.

[5] C. Verhoek, G. I. Beintema, S. Haesaert, M. Schoukens, and R. Tóth, "Deep-learning-based identification of lpy models for nonlinear systems," in *Proc. of the 2022 IEEE 61st Conference on Decision and Control*. IEEE, 2022, pp. 3274–3280.

[6] J. Willard, X. Jia, S. Xu, M. Steinbach, and V. Kumar, "Integrating scientific knowledge with machine learning for engineering and environmental systems," *ACM Computing Surveys*, vol. 55, no. 4, pp. 1–37, 2022.

[7] A. Daw, A. Karpatne, W. D. Watkins, J. S. Read, and V. Kumar, "Physics-guided neural networks (pgnn): An application in lake temperature modeling," in *Knowledge Guided Machine Learning*. Chapman and Hall/CRC, 2022, pp. 353–372.

[8] D. C. Psychogios and L. H. Ungar, "A hybrid neural network-first principles approach to process modeling," *AIChE Journal*, vol. 38, no. 10, pp. 1499–1511, 1992.

[9] J. Pathak, A. Wikner, R. Fussell, S. Chandra, B. R. Hunt, M. Girvan, and E. Ott, "Hybrid forecasting of chaotic processes: Using machine learning in conjunction with a knowledge-based model," *Chaos: An Interdisciplinary Journal of Nonlinear Science*, vol. 28, no. 4, 2018.

[10] T. P. Bohlin, *Practical grey-box process identification: theory and applications*. Springer Science & Business Media, 2006.

[11] R.-S. Götte and J. Timmermann, "Composed physics-and data-driven system identification for non-autonomous systems in control engineering," in *Proc. of the 3rd International Conference on Artificial Intelligence, Robotics and Control*, 2022, pp. 67–76.

[12] B. Sohlberg and E. W. Jacobsen, "Grey box modelling—branches and experiences," *IFAC Proceedings Volumes*, vol. 41, no. 2, pp. 11 415–11 420, 2008.

[13] M. L. Thompson and M. A. Kramer, "Modeling chemical processes using prior knowledge and neural networks," *AIChE Journal*, vol. 40, no. 8, pp. 1328–1340, 1994.

[14] B. Sun, C. Yang, Y. Wang, W. Gui, I. Craig, and L. Olivier, "A comprehensive hybrid first principles/machine learning modeling framework for complex industrial processes," *Journal of Process Control*, vol. 86, pp. 30–43, 2020.

[15] M. Schoukens and R. Tóth, "On the initialization of nonlinear LFR model identification with the best linear approximation," *IFAC-PapersOnLine*, vol. 53, no. 2, pp. 310–315, 2020.

[16] L. Hewing, D. Gramlich, C. Verhoek, J. Veenman, R. Polonio, C. Ardura, R. Tóth, C. Ebenbauer, C. W. Scherer, and V. Preda, "Enhancing the guidance, navigation and control of autonomous parafoils using machine learning methods," in *Proc. of the 12th International Conference on Guidance, Navigation & Control Systems*, 2023, pp. 1–15.

[17] K. Zhou, J. Doyle, and K. Glover, *Robust and Optimal Control*, ser. Feher/Prentice Hall Digital. Prentice Hall, 1996.

[18] R. Tóth, *Modeling and identification of linear parameter-varying systems*. Springer, 2010, vol. 403.

[19] M. Schoukens and R. Tóth, "Linear parameter varying representation of a class of MIMO nonlinear systems," *IFAC-PapersOnLine*, vol. 51, no. 26, pp. 94–99, 2018.

[20] M. Bolderman, H. Butler, S. Koekebakker, E. van Horssen, R. Kamidi, T. Spaan-Burke, N. Stribosch, and M. Lazar, "Physics-guided neural networks for feedforward control with input-to-state-stability guarantees," *Control Engineering Practice*, vol. 145, p. 105851, 2024.

[21] C. Bishop, "Neural networks for pattern recognition," *Clarendon Press google scholar*, vol. 2, pp. 223–228, 1995.

[22] D. Masti and A. Bemporad, "Learning nonlinear state-space models using autoencoders," *Automatica*, vol. 129, p. 109666, 2021.

[23] G. I. Beintema, R. Tóth, and M. Schoukens, "Non-linear state-space model identification from video data using deep encoders," *IFAC-PapersOnLine*, vol. 54, no. 7, pp. 697–701, 2021.